IEEJ Journal of Industry Applications
Vol.8 No.2 pp.256–262 DOI: 10.1541/ieejjia.8.256

Paper

Vibration Suppression in Position Control System by Pole Zero Cancellation using Limited Pole Placement Method

Yoshiyuki Urakawa[*a)] Senior Member

(Manuscript received May 2, 2018, revised Sep. 19, 2018)

Almost all motion control systems have low-stiffness parts, and exhibit resonance characteristics. In many cases, we use the systems at a lower frequency range than the resonant frequency. However, in some cases, we have to use them in the same frequency range as that of the resonance. Various researches have been conducted to suppress the vibration of resonant systems with feedback controllers. They are very effective, but we need to design dedicated controllers with special capabilities. On the other hand, a feedforward controller can change the zeros of the system, which in turn suppresses the vibration. In this paper, two examples that demonstrate the effect of feedforward controllers are introduced. They change the reference response of the systems and the limited pole placement method, which assigns the representative poles precisely, is used to assist the effect.

Keywords: resonant system, feedforward controller, two-mass resonant system, pole zero cancellation, limited pole placement method

1. Introduction

Almost all motion control systems have low-stiffness parts; for example, gears and ball screws are low-stiffness parts of mechanical systems. These low-stiffness parts determine the resonance characteristics of the system. In many cases, we use systems in frequency areas lower than the resonance frequency. In these cases, resonant characteristics are cancelled by notch filters or simply ignored. However, in some cases, we must use them in the same frequency area as the resonance. Various studies have been performed on vibration suppression in resonant systems. Resonant ratio control can change the resonance frequency to make the system robust [(1)–(3)]. Modern control theory and H-infinity control theory are remarkably effective in suppressing vibrations [(4)–(6)]. The use of phase shifters in high-frequency areas makes a system robust despite the presence of several resonance modes [(7)(8)]. Additionally, two-degree-of-freedom (2DOF) controllers can suppress vibrations with their feedforward controllers [(9)–(11)]. Although all of these controllers are highly effective, we must design dedicated controllers with special functionalities. However, a simple 2DOF proportional-integral- derivative (PID) controller can easily change the zeros of the reference transfer function, which can shape the reference response. This is called the pole zero cancellation (PZC) method [(12)], which is expected to suppress vibrations easily.

In this paper, two examples that show the effect of the feedforward controller are presented. The first example is a lens-positioning control system for a mobile phone, which is a spring- mass system in which the lens is held by springs. The second example is a servo system for a robot arm; this is a two-mass resonant system in which the robot arm is linked to a motor with a low-stiffness part. In both cases, the feedforward controllers can shape the reference response of the system with PZC. However, if we apply the control system to a digital system, digital delay for example, zero order hold (ZOH) and calculation delay shift the poles of the system, and the zeros cannot cancel the poles completely. Therefore, the poles of the system should be assigned accurately, even in a digital system. The limited pole placement (LPP) method [(13)(18)], which has been proposed by the author, can assign representative poles precisely. In this study, PZC with the LPP method is investigated.

PZC is explained in Section 2. In Section 3, the lens- positioning control system of a mobile phone is discussed as an example of a spring-mass system, LPP is explained, and the effect of PZC with LPP is demonstrated. In Section 4, a semi-closed control system of a robot arm is discussed as an example of a two-mass resonant system, and it is demonstrated that vibration can be suppressed by PZC, and it is realized by LPP in a digital control system.

2. PZC

2.1 2DOF Control System Control systems use reference signals and plant outputs. Therefore, they can generally be drawn like the block diagram in Fig. 1(a). The output of the controller, u, is generated from a reference signal, r, and the plant output, y. The controller for a feedforward path, C_1, changes a reference transfer function. The controller for a feedback loop, C_2, determines the robustness of the system. The two parts of the controller can change these two properties. The controller C is called the 2DOF controller and can be parameterized by two independent parameters. Thus, we can design two properties independently [(14)(15)]. The block diagram in Fig. 1(a) can be modified to the block

a) Correspondence to: Yoshiyuki Urakawa. E-mail: urakawa.yoshiyuki@nit.ac.jp
* Nippon Institute of Technology
4-1, Gakuendai, Miyashiro-machi, Minami Saitama-Gun, Saitama 345-8501, Japan

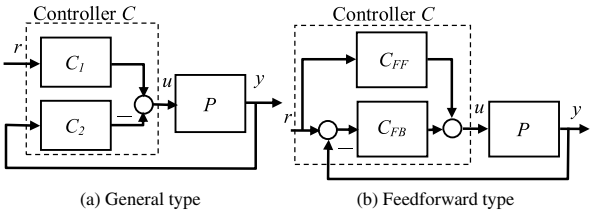

(a) General type (b) Feedforward type

Fig. 1. 2DOF control system

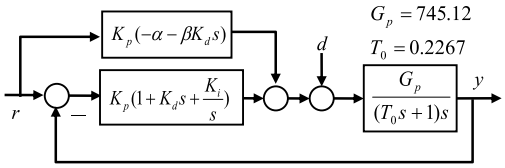

Fig. 2. 2 DOF PID control system

diagram in Fig. 1(b). The controllers in Fig. 1(b) are expressed by Eqs. (1) and (2).

$$C_1 = C_{FF} + C_{FB} \quad \cdots\cdots (1)$$

$$C_2 = C_{FB} \quad \cdots\cdots (2)$$

There are many other possible modifications; for example, filter-type and loop-type. The controllers can be transformed to each other with the method described by Eqs. (1) and (2) [16].

2.2 2DOF PID Controller The feedforward-type 2DOF controller for a PID control system is called the 2DOF PID controller [16][17]. The block diagram of a motor positioning system is shown in Fig. 2. If $\alpha = \beta = 0$, the controller is equivalent to a conventional PID controller. The disturbance transfer function is expressed by Eq. (3) and the reference transfer function by Eq. (4).

$$G_{yd}(s) = \frac{G_p s}{T_0 s^3 + (1 + K_p K_d G_p) s^2 + K_p G_p s + K_p K_i G_p} \quad \cdots\cdots (3)$$

$$G_{yr}(s) = \frac{K_p((1-\beta)K_d s^2 + (1-\alpha)s + K_i) G_p}{T_0 s^3 + (1 + K_p K_d G_p) s^2 + K_p G_p s + K_p K_i G_p} \quad \cdots\cdots (4)$$

2.3 Effect of PZC If we set control parameters in the system of Fig. 2 as $K_p = 82.15$, $K_i = 100$ and $K_d = 0.003317$, the three poles of the closed loop are at -300 ± 0j rad/s. If $\alpha = \beta = 0$, the zeros of the reference transfer function are at -150.7 ± 86.2j rad/s, respectively, according to Eq. (4). The step reference response is shown by the dashed line in Fig. 3. The step response of a conventional PID control system has overshoot, which arises from the zeros. Therefore, we apply PZC with the 2DOF PID controller. If we set $\alpha = 0.3333$ and $\beta = 0.6650$, the zeros are at -300 ± 0j rad/s, and two of the three multiple poles are cancelled. The step response of the 2DOF PID control system is shown in Fig. 3 by the solid line. There is no overshoot and the zeros shape the step response.

Next, we apply PZC to resonant plants. In both cases, the PZC method works well if the poles are assigned accurately with the LPP method.

3. Spring-Mass System

3.1 Lens-Positioning Control System In recent years, image sensors for mobile phones have greatly improved and autofocus systems have begun to be applied. In such systems, the lens position is controlled to focus on the image sensor. Figure 4 shows a diagram of a lens positioning system [18], and Fig. 5 shows the frequency characteristics of a plant with a resonance frequency of 60 Hz. Figure 6 is a block diagram of this example. The sampling frequency is 10 kHz, and the system has three sampling period delays. The digital control parameters K_{pz}, a_z, b_z, and c_z are calculated using the LPP method. (The feedforward controller is explained later in subsection 3.3.)

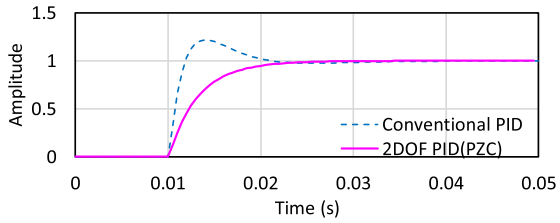

Fig. 3. Step responses of a 2 DOF PID system

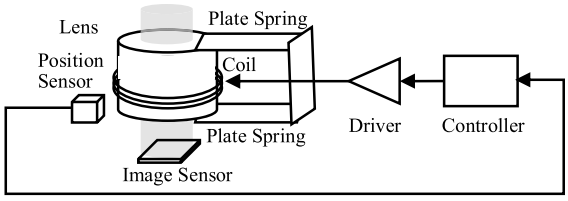

Fig. 4. Schematic of a lens-positioning control system

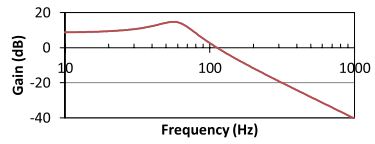

(a) Gain

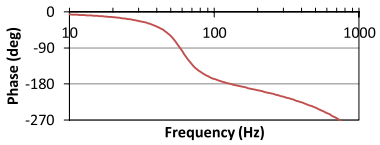

(b) Phase

Fig. 5. Frequency characteristics of the plant

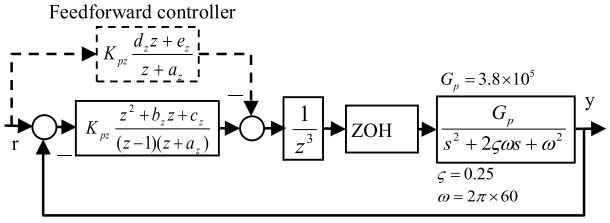

Fig. 6. Block diagram of the lens-positioning control system (discrete)

3.2 The LPP Method The LPP method is used to calculate the parameters of digital controllers. If a digital delay exists, it increases the order of the control system. Therefore, the controller cannot assign all of the poles of the system, because it does not have a sufficient number of parameters. The poles shift to oscillatory positions because the delay introduces a phase lag. With the LPP method, the poles are divided into two groups, the “assigned poles” and the

"determined poles". The assigned poles, whose number is equal to the number of control parameters, are placed exactly, whereas the position of the determined poles is calculated with the control parameters. The exact assigned poles make the system's response less oscillatory, and the determined poles indicate the effect of the delay with their positions. For example, if one of the determined poles is outside the unit circle, it means that the delay makes the system unstable.

The discrete plant, which comes from the plant and the zero- order holder, is expressed by Eq. (5).

$$P(z) = \frac{n_1 z + n_0}{z^2 + d_1 z + d_0} \cdots\cdots (5)$$

where

$$n_1 = 1.8879 \times 10^{-3}$$
$$n_0 = 1.8761 \times 10^{-3}$$
$$d_1 = -1.9799$$
$$d_0 = 0.9813$$

The "fixed part" of the control system, which corresponds to the discrete plant, the delay, and the fixed polynomial of the controller, is expressed by Eq. (6). The "parameter part", which comes from the polynomials with control parameters, is expressed by Eq. (7). The characteristic polynomial, $\gamma(z)$, is expressed by the fixed part and the parameter part in Eq. (8).

$$\begin{aligned}\frac{n(z)}{d(z)} &= \frac{1}{z-1}\frac{1}{z^3}P(z) \\ &= \frac{1}{z-1}\frac{1}{z^3}\frac{n_1 z + n_0}{z^2 + d_1 z + d_0} \\ &= \frac{b_1 z + b_0}{z^6 + a_5 z^5 + a_4 z^4 + a_3 z^3} \cdots\cdots (6)\end{aligned}$$

$$\begin{aligned}\frac{\beta(z)}{\alpha(z)} &= K_{pz}\frac{z^2 + b_z z + c_z}{z + a_z} \\ &= \frac{\beta_2 z^2 + \beta_1 z + \beta_0}{\alpha_1 z + \alpha_0} \cdots\cdots (7)\end{aligned}$$

$$\gamma(z) = \alpha(z)d(z) + \beta(z)n(z) \cdots\cdots (8)$$

If the order of the characteristic polynomial, n_γ, is 7, and the number of parameters is 4, then the number of the assigned poles, n_p, is 4, and that of the determined poles, $n_q = n_\gamma - n_p$, is 3. The four assigned poles are denoted as p_1, p_2, p_3, and p_4 and the three determined poles as q_1, q_2, and q_3. Therefore, the characteristic polynomial, $\gamma(z)$, is expressed in Eq. (9).

$$\begin{aligned}\gamma(z) &= (z-p_1)(z-p_2)(z-p_3)(z-p_4)(z-q_1)(z-q_2)(z-q_3) \\ &= (z^4 + P_3 z^3 + P_2 z^2 + P_1 z + P_0)(z^3 + Q_2 z^2 + Q_1 z + Q_0) \\ &= P_p(z)(z^3 + Q_p(z)) \cdots\cdots (9)\end{aligned}$$

From Eqs. (8) and (9), the Diophantine equation for pole placement is modified as Eq. (10), which is written as Eq. (11) in matrix notation, where θ^T, E, and ψ^T are given by Eqs. (12)–(14). The parameters and the determined poles are derived from the equation $\theta^T = \psi^T E^{-1}$.

$$\alpha(z)d(z) + \beta(z)n(z) - P_p(z)Q_p(z) = z^3 P_p(z) \cdots\cdots (10)$$

$$\theta^T E = \psi^T \cdots\cdots (11)$$

Table 1. Control parameters of the LPP method

τ[s]	0.006	0.004	0.003	0.0023	0.0022
K_{pz}	2.6979	8.3740	20.5926	72.7533	104.5798
a_z	−0.8214	−0.6598	−0.3842	0.6357	1.2349
b_z	−1.9653	−1.9431	−1.9243	−1.9022	−1.8977
c_z	0.9662	0.9448	0.9268	0.9062	0.9021
q_1	0.0615	0.0558	0.0010	−0.2607	−0.2891
q_2	±0.1829j	±0.2875j	±0.4045j	±0.4522j	±0.3798j
q_3	−0.1552	−0.2222	−0.3053	−0.7011	−1.2242

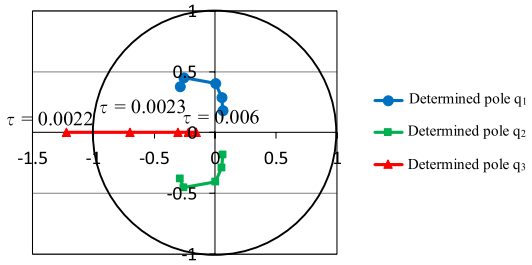

Fig. 7. Positions of determined poles

$$\theta^T = \begin{bmatrix}\alpha_0 & \alpha_1 & \beta_0 & \beta_1 & \beta_2 & Q_0 & Q_1 & Q_2\end{bmatrix} \cdots\cdots (12)$$

$$\psi^T = \begin{bmatrix}0 & 0 & 0 & P_0 & P_1 & P_2 & P_3 & 1\end{bmatrix} \cdots\cdots (13)$$

$$E = \begin{bmatrix} 0 & 0 & 0 & a_3 & a_4 & a_5 & 1 & 0 \\ 0 & 0 & 0 & 0 & a_3 & a_4 & a_5 & 1 \\ b_0 & b_1 & 0 & 0 & 0 & 0 & 0 & 0 \\ 0 & b_0 & b_1 & 0 & 0 & 0 & 0 & 0 \\ 0 & 0 & b_0 & b_1 & 0 & 0 & 0 & 0 \\ -P_0 & -P_1 & -P_2 & -P_3 & -1 & 0 & 0 & 0 \\ 0 & -P_0 & -P_1 & -P_2 & -P_3 & -1 & 0 & 0 \\ 0 & 0 & -P_0 & -P_1 & -P_2 & -P_3 & -1 & 0 \end{bmatrix} \cdots\cdots (14)$$

Table 1 shows the parameters of the digital controller. The pole assignments are determined using the coefficient diagram method [19] in a continuous system. The equivalent time constant, τ, and the stability index, γ_i, define the characteristic polynomials, and the poles can be calculated. The poles are translated to the digital system by $z = e^{st}$. The parameters and the determined poles are calculated using Eqs. (12)–(14). Figure 7 shows the position of the determined poles on the z-plane. The determined pole, q_3, moves in the negative direction, from z = −0.1552 at τ = 0.006 s to z = −0.7011 at τ = 0.0023 s. When τ = 0.0022 s, the determined pole, q_3, exits the unit circle, which means that the system becomes unstable. In other words, τ = 0.0023 s is the bound of the stable system.

3.3 Effect of PZC The closed-frequency characteristic curves of the parameter set obtained from the LPP method (τ = 0.006 s in Table 1) are shown in Fig. 8. The gain characteristic, shown in Fig. 8(a), has a slightly notched curve at 40 Hz. Because the resonance frequency of the plant is close to the zero-cross frequency of the system, the phase of the controller must be advanced steeply at a slightly lower frequency than the resonance frequency. This steep phase advance produces the notched shape in Fig. 8(a), which appears to have an oscillatory step response to the reference.

Figure 9 shows the simulated step response. The dashed line shows that the movement of the lens is oscillatory, which is undesirable for an autofocus actuator. The feedforward

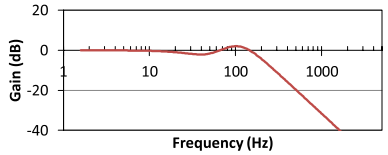

(a) Gain

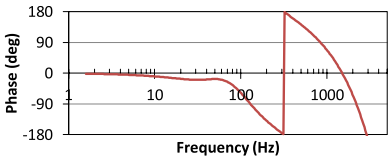

(b) Phase

Fig. 8. Closed-loop frequency characteristic curves

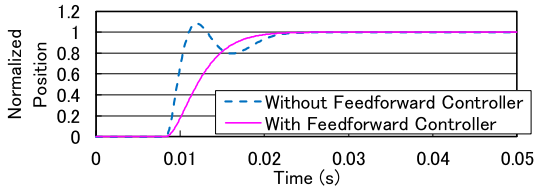

Fig. 9. Reference step response with and without the feedforward controller (simulation)

controller is used to make the response smooth with the PZC method. The dashed-line block in Fig. 6 is a feedforward controller added to a conventional system. The reference transfer function is expressed by Eq. (15).

$$G(z) = \frac{\left(K_{pz}\dfrac{z^2+b_z z+c_z}{(z-1)(z+a_z)} - K_{pz}\dfrac{d_z z+e_z}{z+a_z}\right)\dfrac{1}{z^3}\dfrac{n_1 z+n_0}{z^2+d_1 z+d_0}}{1+K_{pz}\dfrac{z^2+b_z z+c_z}{(z-1)(z+a_z)}\dfrac{1}{z^3}\dfrac{n_1 z+n_0}{z^2+d_1 z+d_0}}$$

$$= \frac{K_{pz}((1-d_z)z^2+(b_z+d_z-e_z)z+(c_z+e_z))(n_1 z+n_0)}{z^3(z-1)(z+a_z)(z^2+d_1 z+d_0)+K_{pz}(z^2+b_z z+c_z)(n_1 z+n_0)} \quad \cdots\cdots (15)$$

The parameters d_z and e_z assign the zeros of the reference transfer function. When the zeros are assigned at p_{z1} and p_{z2}, parameters d_z and e_z are calculated by Eqs. (16) and (17), respectively.

$$d_z = 1 - \frac{1+b_z+c_z}{p_{z1}p_{z2}-(p_{z1}+p_{z2})+1} \quad \cdots\cdots (16)$$

$$e_z = p_{z1}p_{z2}(1-d_z)-c_z \quad \cdots\cdots (17)$$

The assigned poles of $\tau = 0.006$ s are at 0.9576 ± 0.055j and 0.9591 ± 0.013j and the zeros are at 0.9826 ± 0.0249j. The complex zeros at lower position than the poles create the oscillatory step response. Therefore, the zeros should be assigned at 0.9576 ± 0.055j to cancel the poles, and the parameters d_z and e_z are calculated from Eqs. (16), (17) as $d_z = 2.1813$ and $e_z = -2.1315$. The step response is shown by the solid line in Fig. 9, which is smoothed by the feedforward controller.

Figure 10 displays the experimental data. Figure 10(a) shows the step response without a feedforward controller. The experimental data are oscillatory, in agreement with the simulated data. Figure 10(b) shows a step response with a feedforward controller. The response becomes smooth, similar to the simulated data.

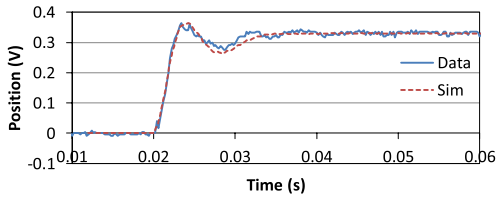

(a) Without feedforward controller

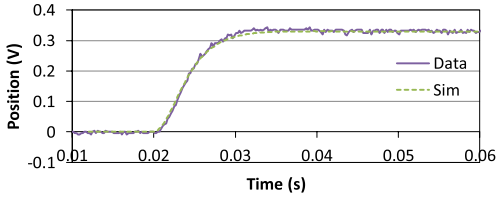

(b) With feedforward controller

Fig. 10. Reference step response with and without a feedforward controller

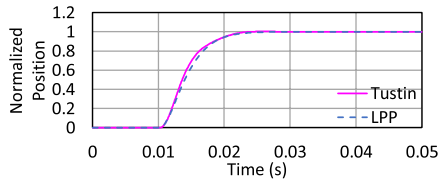

(a) General view

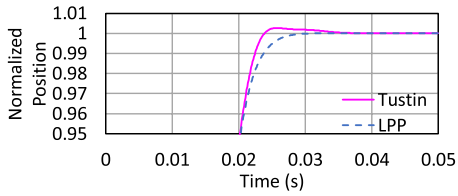

(b) Magnified view

Fig. 11. Reference step response of Tustin transform and LPP method

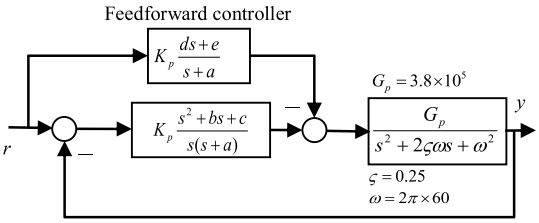

Fig. 12. Block diagram of lens-positioning control system with a feedforward controller (continuous)

3.4 Effect of LPP PZC provides a smooth step response in a spring-mass system. Although it is important to assign the zeros at the same position as the poles, it is rather difficult to assign poles accurately in a digital control system because of digital delay. The LPP method can assign the representative poles accurately, considering the digital delay. However, the Tustin transform, which is the most popular method to translate a continuous controller to a digital controller, cannot account for the digital delay. Step responses are compared in Fig. 11 to show the influence of the digital delay. The step response of the Tustin transform has an overshoot, as shown in Fig. 11(b). The step response is simulated as follows. First, the control parameter set for the continuous lens-positioning control system in Fig. 12 are derived as $K_p = 2.5477$, $a = 1478.2$, $b = 380.8$, $c = 99625$, $d = 0.8017$,

and $e = 215.5$ to assign the poles at -416.7 ± 573.5j and -416.7 ± 135.4j, which correspond to $\tau = 0.006$ s. The zeros are assigned at -416.7 ± 573.5j to cancel two poles. Next, the continuous controller is translated to the digital controller by a Tustin transform, and the parameters are $K_{pz} = 2.4181$, $a_z = -0.8624$, $b_z = -1.9617$, $c_z = 0.9626$, $d_z = 1.9276$, and $e_z = -1.8675$. This parameter set gives the step response in Fig. 11(b). The poles of the digital control system shown in Fig. 6 with this parameter set are 0.9674 ± 0.0172j and 0.9670 ± 0.0719j, and the zeros are 0.9576 ± 0.0550j. This shows that the zeros are set accurately; however, the poles are shifted by the digital delay. Therefore, the zeros cannot cancel the poles completely, which causes the overshoot in Fig. 11(b). Conversely, the LPP method can assign poles accurately and cancel them completely.

4. Two-Mass Resonant System

4.1 Robot-Arm Control System The second example is a servo system for a robot arm, which is a two-mass resonant system. Figure 13 shows the illustrations of two robots. Figure 13(a) displays a conventional selective compliance assembly robot arm (SCARA), and Fig. 13(b) shows the robot used in this experiment, called a "full earthed and balanced" (FEB) robot [20]. Both robots have two arms. The arm connected to the body of the robot is called the 1st arm and that connected to the 1st arm is called the 2nd arm. The two arms of the conventional robot interfere with each other which limits the performance of the robot.

The 2nd arm of the FEB robot is modified to cancel this interference. The 2nd arm has a counter-weight to set the gravity center on the rotation center, and the motor of the 2nd arm is set on the robot's body to receive the reaction torque. Therefore, the two arms of the FEB robot have no interference and can be driven independently.

Figure 14 shows a servo system of the 2nd arm. The angle of the motor, θ_m, is used for a feedback signal and a simple 2DOF PID controller is used. Figure 15 shows the frequency characteristics of the plant. The 2nd arm has a resonance because its counter-weight is heavy, and it is moved with a low-stiffness part. Therefore, the 2nd arm is a typical two-mass resonant system. Its resonance characteristics are derived from the measured data. If we ignore the resonance and assume the system to be the one-mass system of Fig. 2, then $G_p = 71.07$ and $T_0 = 0.2067$ (dashed line in Fig. 15).

First, we calculate the control parameters with a direct method, assuming that the system is the one-mass system shown in Fig. 2. The poles and zeros are assigned multiples at -50 rad/s, -100 rad/s, -150 rad/s, -200 rad/s, and -300 rad/s. Figure 16 shows the complementary sensitivity functions of the servo system in Fig. 14 with each parameter set. All systems are stable despite the resonance. However, the reference response is not good. For example, the simulated position response of the parameter set for -200 rad/s ($K_p = 604.1$, $K_i = 66.7$, $K_d = 0.00496$, $\alpha = 0.333$, and $\beta = 0.664$) to a trapezoidal velocity curve is shown in Fig. 17(a), with the positions of the motor and the arm. The latter is oscillating owing to the resonance at approximately 15 Hz.

Next, we apply the PZC method to the system. The oscillating pole is simulated as -2.76 ± 101.18j. To assign the zeros at the oscillating poles, α should be 0.9640, and β should be -0.3121, according to the direct method and Eq. (4). The simulated data shown in Fig. 17(b) demonstrate that the

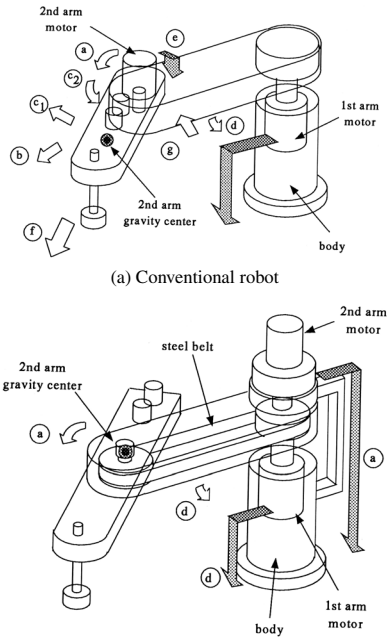

(a) Conventional robot

(b) Full earthed and balanced (FEB) robot

Fig. 13. SCARA-type industrial robot

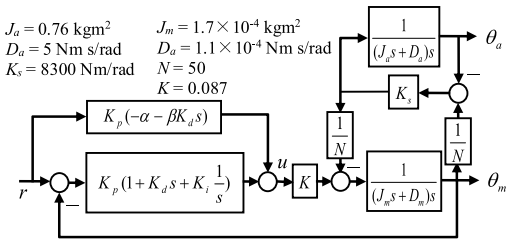

Fig. 14. Servo system of the 2nd arm

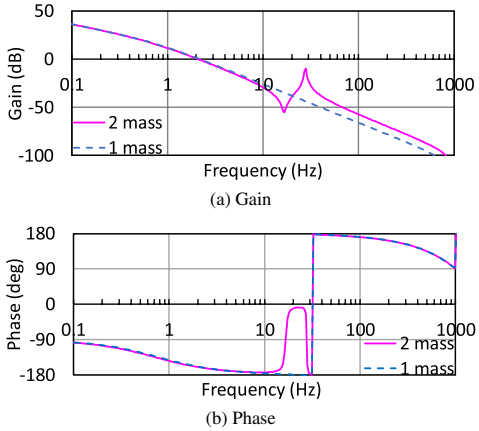

(a) Gain

(b) Phase

Fig. 15. Frequency characteristics of the plant

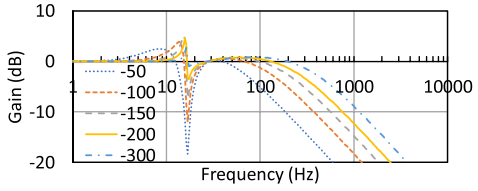

Fig. 16. Complementary sensitivity functions

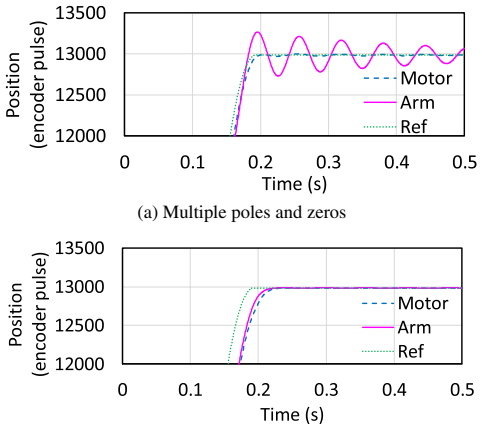

(a) Multiple poles and zeros

(b) PZC method (zeros are assigned at oscillating poles)

Fig. 17. Simulated position response (continuous system)

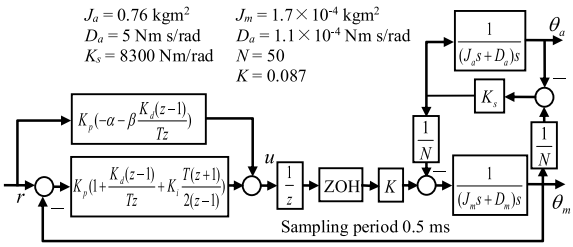

Fig. 18. Digital control system of the 2nd arm

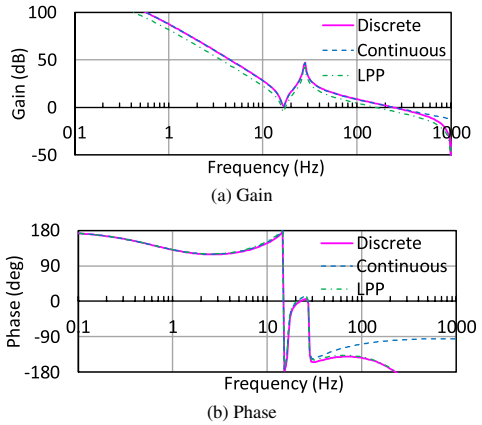

(a) Gain

(b) Phase

Fig. 19. Open-loop frequency characteristics

oscillation disappears.

4.2 Digital System To confirm the effect of the PZC method experimentally, we apply the PZC parameters to a digital control system. The block diagram of the digital control system is shown in Fig. 18. The sampling period is 0.5 ms, and the system has one sampling period delay. The open-loop frequency characteristics are shown in Fig. 19 (solid line). The simulated data of the continuous system are also shown by the dashed line as a reference. The gain and phase margin of the solid line is too small to operate in the experimental setup. The simulated data of the continuous system(dashed lines) have sufficient margin because there is no phase delay in the high-frequency area. In other words, the digital control system becomes unstable because of the digital delay.

Therefore, we attempt to apply the LPP method to a digital servo system (Fig. 20). We assume the system to be a

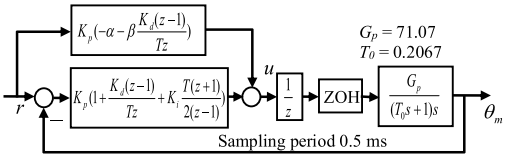

Fig. 20. Digital control system for LPP

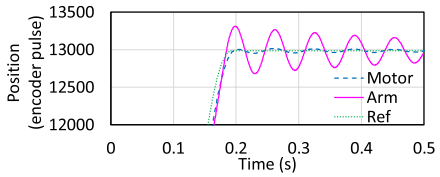

(a) Multiple poles and zeros

(b) PZC method (zeros are assigned at oscillating poles)

Fig. 21. Simulated position response (discrete system)

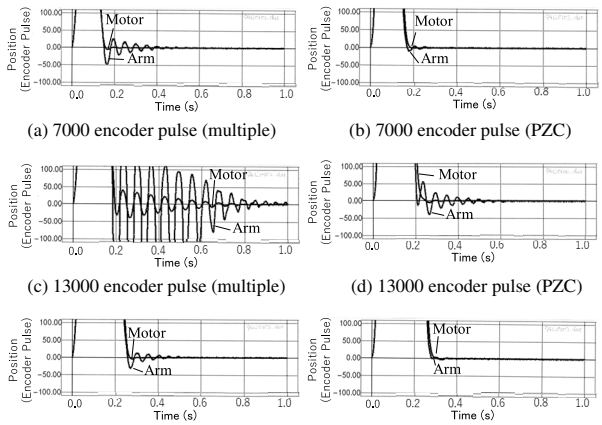

(a) 7000 encoder pulse (multiple)

(b) 7000 encoder pulse (PZC)

(c) 13000 encoder pulse (multiple)

(d) 13000 encoder pulse (PZC)

(e) 22000 encoder pulse (multiple)

(f) 22000 encoder pulse (PZC)

Fig. 22. Reference response for trapezoidal velocity trajectory

one-mass system similar to the continuous system. The parameters for −200 rad/s are $K_p = 332.5$, $K_i = 61.7$, $K_d = 0.00571$, $\alpha = 0.398$, and $\beta = 0.6756$. The open loop frequency characteristics are drawn in Fig. 19 (dash-dotted line). The gain decreases, and the margins increase. The reference response is plotted in Fig. 21(a), which shows that the oscillation is almost the same as in Fig. 17(a). The oscillating pole is simulated as −2.49±98.60j. To cancel these poles, α should be 0.9838 and β should be −0.1100. The simulated data are shown in Fig. 21(b). The oscillation disappears, similar to the continuous system in Fig. 17(b).

Next, the parameter set by PZC is applied to the experimental setup. The error signals are shown in Fig. 22. The error signal of the motor is calculated from the encoder data and that of the arm from the measured data, obtained using an eddy current position sensor at the target point. The moving distance is 7000 encoder pulses, 13000 encoder pulses, and 22000 encoder pulses. The multiple zero assignments and the zero assignments by PZC are compared. The amplitude of the vibration differs according to the moving distance

owing to the frequency component of the reference signals. If the reference signal contains many frequency components around the resonance frequency, the vibration increases significantly. However, at each distance, the amplitude of zeros assigned with PZC is obviously smaller. The parameter set by the PZC method can suppress the vibration and the LPP method enables the application of pole assignment in the experimental setup.

5. Conclusion

Vibration suppression by the PZC method is investigated. A simple 2DOF PID controller is used for PZC to move zeros of a reference transfer function. The PZC method is applied to a spring-mass system and a two-mass resonant system to suppress vibrations and is confirmed to be effective in both cases. If we apply the PZC method to a digital control system, accurate pole assignment is important. The LPP method is also confirmed to improve accurate pole assignment in digital systems for PZC.

In this paper, the robustness of the vibration suppression achieved by PZC are not discussed.

References

(1) N. Matsui and Y. Hori: “Advanced Technologies in Motor Control”, T. IEE Japan, Vol.113-D, No.10, pp.1122–1137 (1993) (in Japanese)

(2) K. Yuki, T. Murakami, and K. Ohnishi: “Vibration Control of a 2 Mass Resonant System by the Resonance Ratio Control”, T. IEE Japan, Vol.113-D, No.10, pp.1162–1169 (1993) (in Japanese)

(3) Y. Hori: “2-Inertia System Control using Resonance Ratio Control and Manabe Polynomials”, T IEE Japan, Vol.114-D, No.10, pp.1038–1045 (1994) (in Japanese)

(4) Y. Hori: “2-Mass System Control based on Load-Side Acceleration Control and State Feedback”, T IEE Japan, Vol.112-D, No.5, pp.499–500 (1992) (in Japanese)

(5) S. Ouchi, T. Mita, and K. Yano: “Active Vibration Control of a Motor System by Using H∞ Control”, T. IEE Japan, Vol.113-D, No.3, pp.325–332 (1993) (in Japanese)

(6) K. Nonami and T. Mita: “Vibration Control Using H∞ Control”, IRSJ, Vol.13, No.8, pp.29–35 (1995) (in Japanese)

(7) T. Atsumi, T. Arisaka, T. Shimizu, and T. Yamaguchi: “A Method of Designing a Vibration-Servo-Control System to Reduce the Effect of Mechanical Resonant Modes in a Hard Disk Drive”, Trans. Of JSME Series C, Vol.68, No.675, pp.3298–3305 (2002) (in Japanese)

(8) N. Hirose, M. Iwasaki, M. Kawafuku, and H. Hirai: “Robust Vibration Suppression of Resonant Modes by Feedback Compensation Realized Using Allpass Filters”, IEEJ Trans. IA, Vol.129, No.10, pp.981–988 (2009) (in Japanese)

(9) M. Hirata, K.Z. Liu, and T. Mita: “A Design method for Two-Degree-of-Freedom Controller using the Dynamical Model of the Feedback Controller”, T. IEE Japan, Vol.116-D, No.1, pp.71–78 (1996) (in Japanese)

(10) T. Miyazaki, S. Ohtaki, S. Tungpataratanawong, and K. Ohishi: “High Speed Motion Control Method of Industrial Robot Based on Dynamic Torque Compensation and Two-Degree-of-Freedom Control System”, IEEJ Trans. IA, Vol.123, No.5, pp.525–532 (2003) (in Japanese)

(11) K. Ito, R. Nagata, M. Iwasaki, and N. Matsui: “GA-Based Autonomous Design of Robust Fast and Precise Positioning Considering Machine Stand Vibration Suppression”, IEEJ Trans. IA, Vol.124, No.6, pp.607–616 (2004) (in Japanese)

(12) A. Takano: “Two-Degrees-of-Freedom Self-Tuning Control for Motor Drives Using Pole-Zero Cancellation Method”, IEEJ Trans. IA, Vol.129, No.4, pp.415–422 (2009) (in Japanese)

(13) Y. Urakawa: “Parameter Design for a Digital Control System with Calculation Delay Using a Limited Pole Placement Method”, IEEJ Trans. IA, Vol.133, No.3, pp.272–281 (2013) (in Japanese)

(14) T. Sugie and T. Yoshikawa: “Basic Structure of Two-Degree-of-Freedom Control Systems with Its Application to Servo Problem”, T. SICE, Vol.22, No.2, pp.156–161 (1986) (in Japanese)

(15) S. Hara and T. Sugie: “Control Systems with Two Degree of Freedom II”, Journal of System and Control, Vol.30, No.8, pp.457–466 (1986) (in Japanese)

(16) M. Araki: “Control Systems with Two Degree of Freedom I”, Journal of System and Control, Vol.29, No.10, pp.649–656 (1985) (in Japanese)

(17) H. Taguchi, M. Doi, and M. Araki: “Optimal Parameters of Two-Degrees-of-Freedom PID Control Systems”, T. SICE, Vol.23, No.9, pp.889–895 (1986) (in Japanese)

(18) Y. Urakawa: “Lens Position Control System Using Limited Pole Placement Method”, IEEJ Journal IA, Vol.6, No.2, pp.117–123 (2016)

(19) S. Manabe: “Controller Design of Two-Mass Resonant System by Coefficient Diagram Method”, T. IEE Japan, Vol.118-D, No.1, pp.58–66 (1998)

(20) A. Kimura, I. Itoh, M. Tominaga, S. Itoh, H. Takizawa, T. Nakamura, T. Kusano, Y. Urakawa, N. Mukai, and H. Yamada: “Development of a High Speed Horizontally Jointed Robot (Full Earthed and Balanced Robot)”, Proc. Sony Res. Forum, Vol.5, pp.527–532 (1996)

Yoshiyuki Urakawa (Senior Member) received a B.Eng. degree from the Department of Mathematical Engineering and Information Physics, University of Tokyo, in 1983. He joined Sony in 1983 and his work includes the signal processing of digital video tape recorders, parameter design research for industrial robotics, and the design of a servo system for optical disk drives. He received a D.E. degree from Yokohama National University in 2013. He was transferred to the Nippon Institute of Technology in 2017. His interests are motion control and high-performance servo systems.